Title

Chromohalobacter salixigens uronate dehydrogenase: Directed evolution for improved thermal stability and mutant CsUDH-inc X-ray crystal structure

Authors

Wagschal, Kurt

Chan, Victor J

Pereira, Jose H

et al.

Publication Date

2022-03-01

DOI

10.1016/j.procbio.2020.02.013

Peer reviewed

Contents lists available at ScienceDirect

Process Biochemistry

journal homepage: www.elsevier.com

Chromohalobacter salixigens uronate dehydrogenase: Directed evolution for improved thermal stability and mutant CsUDH-inc X-ray crystal structure

Kurt Wagschal [a,*], Victor J. Chan [a], Jose H. Pereira [b], Peter H. Zwart [c], Banumathi Sankaran [d,*]

[a] USDA Agricultural Research Service, Western Regional Research Center, Albany, CA 94710, USA
[b] Molecular Biophysics and Integrated Bioimaging, Joint BioEnergy Institute, Emeryville, CA, 94608, USA
[c] Molecular Biophysics and Integrated Bioimaging & Center for Advanced Mathematics for Energy Research Applications, Lawrence Berkeley National Laboratories,1 Cyclotron Road, Berkeley, CA, 94703, USA
[d] Molecular Biophysics and Integrated Bioimaging, Berkeley Center for Structural Biology, Lawrence Berkeley National Laboratory, Berkeley, California, 94720, USA

ARTICLE INFO

Keywords:
Uronate dehydrogenase
Directed evolution
Pectin
Alginate
Gene shuffling
Protein thermal stability

ABSTRACT

Chromohalobacter salixigens contains a uronate dehydrogenase termed CsUDH that can convert uronic acids to their corresponding C1,C6-dicarboxy aldaric acids, an important enzyme reaction applicable for biotechnological use of sugar acids. To increase the thermal stability of this enzyme for biotechnological processes, directed evolution using gene family shuffling was applied, and the hits selected from 2-tier screening of a shuffled gene family library contained in total 16 mutations, only some of which when examined individually appreciably increased thermal stability. Most mutations, while having minimal or no effect on thermal stability when tested in isolation, were found to exhibit synergy when combined; CsUDH-inc containing all 16 mutations had $\Delta K_t^{0.5}$ +18 °C, such that k_{cat} was unaffected by incubation for 1 h at ~70 °C. X-ray crystal structure of CsUDH-inc showed tight packing of the mutated residue side-chains, and comparison of rescaled B-values showed no obvious differences between wild type and mutant structures. Activity of CsUDH-inc was severely depressed on glucuronic and galacturonic acids. Combining select combinations of only three mutations resulted in good or comparable activity on these uronic acids, while maintaining some improved thermostability with $\Delta K_t^{0.5} \sim +$ 10 °C, indicating potential to further thermally optimize CsUDH for hyperthermophilic reaction environments.

1. Introduction

The enzymatic conversion of sugars and sugar derivatives from biomass to value added products offers an important route to reducing the environmental and economic impact of food waste [1]. Increasing use of resources such as sugar acids in materials otherwise considered food processing waste that are renewable can increase crop economic value for farmers and processors, as well as being a chemical platform that is non-toxic and readily degraded when released in wastewater streams, thereby facilitating the protection of community safe water supplies and aquatic ecosystems as the use of chemicals released into waste water increases alongside global increases in human population, lifespan, and living standards [2]. Moreover, production of bioproducts from food processing waste rather than food crops does not cause additional land or food use and the concomitant problem of increased natural resource pressure on our common food and arable land resources [3]. The world-wide yearly ~1.7×10^6 metric tons production of orange juice (https://apps.fas.usda.gov/psdonline/circulars/citrus.pdf) generates significant food processing waste that can be a disposal problem, which could be lessened both by generating new products [4] and where applicable increasing its use as a soil amendment [5]. Dried citrus peel contains ~27 % D-galacturonic acid (GalUA), the main alduronic acid component of pectin [6]. Likewise, the pulp waste steam from sugar beet refining, with worldwide production estimated to be ~ 250×10^6 metric tons, contains ~24 % pectin [7]. Brown algae contain as the major cell wall components the C-5 epimeric alduronic acids β-D-mannuronic and α-L-guluronic acid [8]. The C-4 epimeric alduronic acids D-glucuronic acid (GluUA) and D-GalUA (GalUA) can be converted to their respective diacids D-glucaric acid (saccharic acid) and meso-galactaric acid (mucic acid) by the action of uronate dehydrogenases (UDH, EC 1.1.1.203), that oxidize the alduronic acids to the 1,4-lactone product, which hydrolyzes to the linear molecule under basic conditions to render the reaction non-reversible [9]. Aldaric acids are of commercial interest and are listed as a top 10 DOE biomass platform chemical [10] that can be used as chelating agents [11] and in synthetic polymers [12,13]. An engineered *in vivo* metabolic pathway incorporating UDH from *Psuedomonas syringae* has been developed for the production of D-glucaric acid [14], and fungal and yeast strains have been engineered for conversion of D-GalUA to mucic acid [15,16]. Alternatively, *in vitro* biosyn-

* Corresponding authors.
Email addresses: kurt.wagschal@ars.usda.gov (K. Wagschal); bsankaran@lbl.gov (B. Sankaran)

https://doi.org/10.1016/j.procbio.2020.02.013
Received 16 September 2019; Received in revised form 10 February 2020; Accepted 13 February 2020
Available online xxx
1359-5113/

thetic routes in general can have advantages to their living-cell counterparts [17,18]. Thus, as noted previously for UDH catalyzed oxidation of uronic acids GalUA, GluUA, and C-5 isomer D-mannuronic acid by related UDH enzymes [19], *in vitro* production of aldaric acids obviates cellular membrane transport of substrates and products and associated limitations. Moreover, mucic acid is nearly insoluble in water, a potential problem for cell viability and optimum *in-vivo* production [20], while conversely for *in-vitro* production and downstream process development, insolubility provides a basis for readily scaleable product precipitation and crystallization as isolation and purification processes [20].

Improved thermal stability of the enzyme catalysts can increase robustness of industrial processes employing *in vitro* biosynthetic pathways, and accordingly the UDH from *Agrobacterium tumefaciens* (AtUDH) has previously been engineered for increased thermal stability by a semi-rational approach [21]. Natural selection based on heritable expressed material has been exposited as the source of observed species and individual diversity in whole organisms [22], while enzyme directed evolution (DE) encompasses mutation of isolated gene DNA sequences *in-vitro*, followed by expression and selection of encoded mutated protein structures with desired properties [23,24]. Enzyme library diversity can be achieved using error prone PCR and single-gene shuffling [25], and improved upon by gene family shuffling which employs the power of sexual recombination to explore sequence space using *in vitro* recombination by random fragmentation and reassembly of gene families [26–28]. Directed evolution has previously been used for engineering enzyme thermal stability [29]. We describe DE of the UDH from *Chromohalobacter salixigens* (CsUDH, PDB ID 3AY3) using gene family shuffling with UDH enzymes from *Polaromonas naphthalenivorans* CJ2 (PnUDH, NCBI accession ABM36905) and *Pseudomonas syringae* (PsUDH, NCBI accession EU377538), and provide X-ray crystal structure results for the most thermally stabilized mutant termed CsUDH-inc.

2. Materials and methods

2.1. Gene family shuffling DNA library

The DNA sequence alignment of *CsUDH*, *PnUDH*, and *PsUDH* was previously maximized by inspection to encourage homologous recombination, with the stipulation that amino acid sequences remain unaltered and disallowing internal *NdeI* or *XhoI* restriction sites (Fig. 1) [30]. The resulting DNA sequences were synthesized (Genscript USA Inc., Piscataway, NJ) and subcloned into pET29b(+) expression vector (EMD Millipore, Burlington, MA). DNA shuffling was performed as described [27,28], with modification as previously described [31]. Gene shuffled libraries were purified on 0.8 % agarose gels, isolated (Zymo Research Corp., Irvine CA), subcloned into *NdeI*/*XhoI* restriction sites of pET29b(+), and transformed into electrocompetent *E. coli* BL21DE3 cells (Lucigen Corp., Middleton, WI, USA).

2.2. Shuffled library live/dead high throughput screen

Shuffled libraries were plated onto 22 × 22 cm Q-trays (Molecular Devices LLC, Sunnyvale, CA) containing LB agar with 30 μg/ml kanamycin (LB_{Kan}) and grown overnight at 30 °C. Colonies were transferred using a Q-pix robot (Molecular Devices LLC) to 384-well plates containing Overnight Express Autoinduction System 2 (EMD Millipore) supplemented with 25 μg/ml kanamycin, which is a minimal media with low absorption at 340 nm to allow a subsequent 1° live/dead assay screen to be performed in the same plate. Picked plates were grown overnight at 30°C and 500 rpm, and a 384-pin replicator (Boekel Scientific, Feasterville, PA) was used to create shuffled library archive plates using LB_{kan} and 10 % glycerol as cryoprotectant, which were grown overnight as before and stored at -80°C. Induced cultures in the original 384-well plates were lysed and assayed by adding 20 μl of a combined lysis/assay 5x cocktail. Lysis was achieved using final concentrations of 0.25 mg/ml Polymyxin B sulfate (Sigma-Aldrich, St. Louis, MO) and 1 μl/ml Protease Inhibitor III (Pierce Chemical Co., Dallas, TX). Assay component final concentrations were 3 mM NAD, 15 mM glucuronic acid, 50 mM Na phosphate, pH 8.0, 1 mg/ml BSA (Sigma-Aldrich). Immediately after adding the combined lysis/assay buffer, plates were shaken 15 s, and 60 min endpoint absorbance measured at 340 nm. Library clones that showed activity in the 1° screen were re-arrayed by transferring 10 μl from 384-well archive plates to create 96-well 1° screen hit archive plates containing 140 μl LB_{Kan} and 8% glycerol, each with 6 positive (CsUDHwt) and 6 negative (vector only) control wells. These were shaken at 500 rpm overnight at 30 °C, and stored at −80 °C.

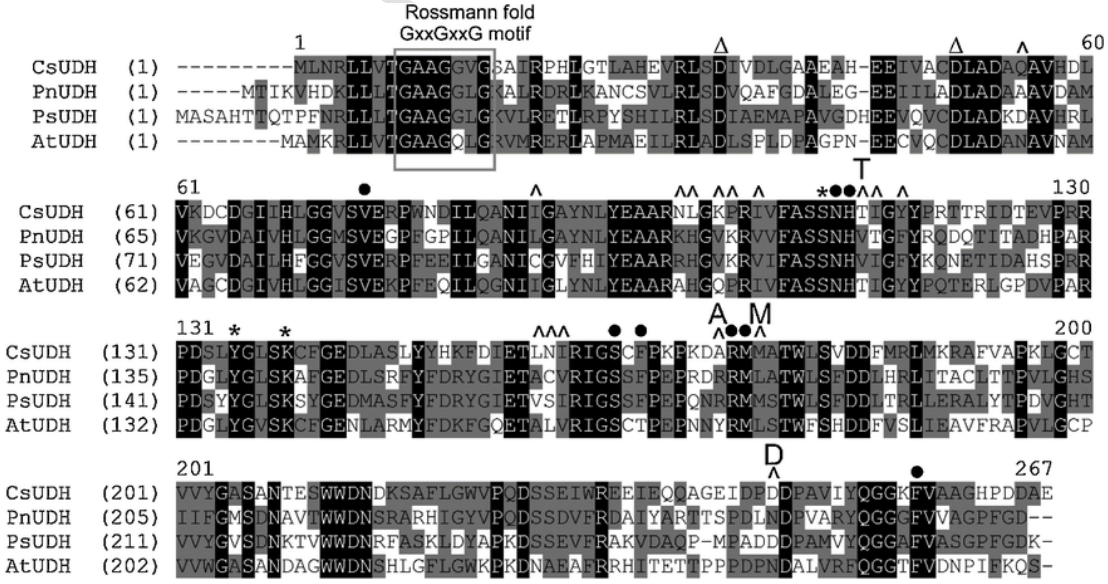

Fig. 1. Amino acid alignment of CsUDH, PnUDH, PsUDH, and AtUDH.Amino acid sequence alignment after [35]. Black background, identical for all enzymes; grey background, identical or similar for two or more enzymes; Rossmann fold GxxGxxG motif, grey box; NAD + binding residues, Δ; catalytic residues TyrxxxLys and Ser, *; substrate binding residues, ●; mutations in thermal stability screening hits (this study), ^; **T** = T113 V; **A** = A172 V; **M** = M175 L; **D** = D246 N. CsUDH, *Chromohalobacter salixigens* uronate dehydrogenase; PnUDH, *Polaromonas naphthalenivorans* uronate dehydrogenase; PsUDH, *Pseudomonas syringae* uronate dehydrogenase; AtUDH, *Agrobacterium tumefaciens* uronate dehydrogenase.

2.3. Shuffled library thermal stability high throughput screen

A 2° thermal stability screen was performed by using a 96-pin replicator (Boekel Scientific) to replicate the 1° screen archive hit plates to 2 ml deep well plates containing 1 ml TB media supplemented with Overnight Express System 1 and 100 ug/ml kanamycin, incubated overnight at 30 °C, 500 rpm. Induced cultures were pelleted and drained. Cell pellets were lysed by adding 200 ul of 1 mg/ml Polymyxin B sulfate, 5 U/ml Benzonase (Sigma-Aldrich), 0.5 mg/ml hen egg white lysozyme, 10 % glycerol, 50 mM Na phosphate, pH 8.0 and 1 ul/ml Protease Inhibitor III and shaking 20 min. The resulting crude enzyme lysate was clarified by centrifuging 10 min at 2400 x g, transferred to new 96-well V-bottom polypropylene plates, and stored at −80 °C. The thermal stability screen was performed in two parts comprised of a screen performed at a single elevated temperature followed by evaluation of the survivors using a temperature gradient. The initial 2° thermal stability challenge screen at a single temperature was performed in 96-well spectrophotometric assay plates by transferring 10 ul aliquots of the crude enzyme lysates to 180 µl assay buffer containing 3 mM NAD, 15 mM glucuronic acid, 50 mM Na phosphate, pH 8.0, 1 mg/ml BSA, and ΔOD_{340nm} measured to determine initial activity. 50 ul aliquots were transferred to PCR strip-tubes for thermal challenge at 68 °C for 1 h, followed by12 °C 10 min, and 30 °C 30 min to allow protein refolding. 10 µl of the thermally challenged lysate was assayed as above. Those clones with residual activity were pursued as potential 2° screen hits, and were individually evaluated at multiple temperatures to generate thermal denaturation curves for determination of $K_t^{0.5}$, the temperature at which activity decreases by 50 % during the thermal challenge. 10 µl aliquots of selected hits were transferred from an archive plate to 10 ml TB_{kan} in Overnight Express System 2 in 50 ml followed by overnight growth and expression as before. Induced cultures were pelleted and lysed in 2 ml CelLytic B (Sigma-Aldrich) supplemented with 0.5 mg/ml lysozyme, 0.2 U/ml Benzonase, 1 ul/ml Protease Inhibitor III and 10 mM β-mercaptoethanol. 25 µl of clarified lysate was diluted in 3 mM NAD, 50 mM Na phosphate, pH 8.0, 0.5 mg/ml BSA and added to each of 12 wells of a PCR plate and subjected to a thermal gradient from 55 °C to 70 °C for 1 h, 12 °C 10 min, and 30 °C 30 min recovery. 10 µl of thermally challenged lysate was assayed in 180 µl assay buffer as above. $K_t^{0.5}$ was determined from the fraction peptide folded using the Boltzmann distribution equation in Prism 6 software package (GraphPad Software, San Diego, CA).

2.4. Recombinant protein expression and purification

CsUDHwt, hits from HTP thermal stability screening of the shuffled DNA library (Table 1), and subsequent CsUDH variant enzymes created using site-specific mutagenesis (Genscript USA, Inc.) containing indicated single and multiple mutations (Tables 2 and 3) were individually expressed and purified for determination of relative thermal stability ($\Delta K_t^{0.5}$) and Michaelis-Menten steady-state kinetic parameters (k_{cat}, K_m). Glycerol stock stabs were used to inoculate Overnight Express Autoinduction System 2 100 ml TB cultures (30 µl/ml kanamycin), grown overnight at 30°. Pelleted cells were lysed using a solution of 65 ml per 5 g Cellytic B, supplemented to contain 0.5 mg/ml hen egg white lysozyme, 2 mm β-mercaptoethanol, 5 U/ml Benzonase, and Protease Inhibitor III. Enzyme was recovered from cell lysate and His-tag affinity chromatography performed using Qiagen Ni-NTA Superflow resin according to manufacturer's instructions (Qiagen, Valencia, CA). A final size-exclusion chromatography purification step was performed using a Tricorn 10/300 Gl Superdex 200 column (GE Healthcare, Chicago, USA) and running buffer consisting of 50 mM $NaHPO_4$ pH 8.0, 150 mM NaCl, and 10 % glycerol, with protein concentration determined spectrophotometrically from absorbance at 280 nm, and aliquots were frozen and stored at −80 °C. SDS-PAGE analysis of CsUDH*wt* and mutant proteins (Fig. 2) was performed using Novex Sharp pre-stained size markers, NuPAGE 4–12 % Bis-Tris 1.0 mm gels, MOPS SDS running buffer, and Simply Blue staining as described by the manufacturer (all from Thermo Fisher Scientific, Waltham, MA).

Table 1
Gene shuffled Library thermal stability hits.

Library Hit	$\Delta K_t^{0.5}$ [a]	Amino acid mutations (total #)
33F2 [d]	3.06 ± 0.57	I88 L; T113 V; I114 T; Y116 F; CsUDH158 [b] (7)
16B3 [d]	5.49 ± 0.59	CsUDH99 [c], T113 V; I114 T (7)
2F10 [d]	5.62 ± 0.77	I88 L; CsUDH99 [c], T113 V; I114 T; Y116 F (9)
21F3 [d]	8.00 ± 0.55	T113 V; D246 N (2)
2D11 [e]	7.67 ± 0.35	Q55R; A172 V; M175 l (3)

[a] $K_t^{0.5}$ = temperature at which ½ initial activity remains after 1 h incubation.
[b] Mutation CsUDH158 = L158A, N159C, and I160V.
[c] Mutation CsUDH99 = N99 K, L100H, K102 V, P103 K, I105V.
[d] Relative to CsUDH (wild-type) $K_t^{0.5}$ = 58.86 ± 0.55 °C.
[e] Relative to CsUDH (wild-type) $K_t^{0.5}$ = 57.03 ± 0.35 °C.

Table 2
Relative thermal stability of mutants from saturation mutagenesis of native Met175 and Asp246.

M175 mutation	$\Delta K_t^{0.5}$ [a] (°C)	D246 mutation	$\Delta K_t^{0.5}$ (°C)
L [b]	+1.5	W	+7.6
F	−9.2	N [b]	+7.5
C	−9.3	K	+7.4
G	−9.8	H	+6.9
W	−10.6	M	+6.1
I	−10.7	Y	+6.0
T	−11.1	Q	+5.5
V	−14.2	F	+5.4
A	−16.6	S	+4.8
Y	−17.2	R	+4.3
S	−20.1	V	+4.3
		C	+4.2
		T	+4.2
		L	+4.1
		A	+3.4
		G	+3.2
		E	+0.3
		I	0.0

[a] $K_t^{0.5}$ = temperature at which ½ initial activity remains after 1 h incubation.
[b] Mutation in thermal stability hits (this study).

2.5. Enzyme thermal stability determination and Michaelis-Menten kinetic parameters

Reported $K_t^{0.5}$ values (Fig. 3, Tables 2 and 3) were obtained using a thermal gradient on a PCR machine consisting of 12 temperature values, ranging from either 46–70 °C for less stable enzymes or 58–82 °C for more stable enzymes. Triplicate assays were performed in PCR strip-tubes containing 190 µl enzyme/assay buffer cocktail containing 100 mM $NaHPO_4$, pH 8.0, 4 mM NAD, and ~2.5 µM enzyme. These were thermally challenged for 1 h, then refolding was allowed to take place by cooling to 12 °C for 5 min, then 30 °C for 15 min. Aliquots were tested for residual activity in 96-well flat polycarbonate assay plates using an assay buffer cocktail consisting of 100 mM $NaHPO_4$, pH 8.0, 4 mM NAD, and 20 mM GluUA, with NAD^+ reduction assessed by measuring ΔOD 340 nm during the ~5 min initial reaction. $K_t^{0.5}$ was calculated by fitting the data from at least two experiments to the Boltzmann distribution equation within Prism 6 (GraphPad Software). Reported kinetic parameters (Table 3) were obtained from at least 2 experiments performed using 8 different substrate concentrations from 0.078 mM to 50 mM, employing triplicate assays at 25 °C using 100 mM phosphate buffer pH 8.0, 1 mg/ml bovine serum albumin, 4 mM NAD, and ~ 2.5 nM enzyme such that < 10 % GalUA and GluUA substrate conversion occurred for all tested substrate concentrations during the initial ~3 min portion of the assay. ΔOD (340 nm) was determined using a Spectramax M3 plate reader (Molecular Devices), and the data fitted to the Michaelis-Menten equation $v/E_t = k_{cat}S/K_m + S$ using Prism 6 (GraphPad Software).

Table 3
Thermal stability $K_t^{0.5}$ [a] and Michaelis-Menten kinetic parameter values for enzymes acting on glucuronic acid (GluUA) and galacturonic acid (GalUA) at 25 °C.

			GluUA			GalUA		
Enzyme	$K_t^{0.5}$ [a] (°C)	$\Delta K_t^{0.5}$ (°C)	k_{cat} (s^{-1})	K_m (mM)	k_{cat}/K_m (s^{-1} mM^{-1})	k_{cat} (s^{-1})	K_m (mM)	k_{cat}/K_m
CsUDHwt[b]	57.1 ± 0.4	0	263 ± 5	1.6 ± 0.6	161 ± 23	30.8 ± 1.4	0.18 ± 0.04	172 ± 35
CsUDH mutation (Abbreviation)								
Q55R	57.2 ± 0.3	0.02 ± 0.4	270 ± 12	1.7 ± 0.1	161 ± 11	28 ± 1.4	0.19 ± 0.03	153 ± 24
I88L	56.2 ± 0.2	−1.0 ± 0.4	192 ± 7	1.5 ± 0.1	125 ± 8	22 ± 1.1	0.20 ± 0.02	112 ± 14
CsUDH99[c]	58.0 ± 0.5	0.8 ± 0.6	142 ± 7	0.9 ± 0.02	162 ± 9	17 ± 0.97	0.13 ± 0.01	125 ± 10
T113 V (T)	60.2 ± 0.01	3.1 ± 0.4	192 ± 6	1.7 ± 0.05	115 ± 4.8	20 ± 0.81	0.15 ± 0.01	132 ± 10
I114T	57.3 ± 0.4	0.2 ± 0.6	155 ± 6	3.2 ± 1.1	48 ± 17	17 ± 0.33	0.41 ± 0.13	41 ± 14
Y116 F (Y)	58.0 ± 0.3	0.9 ± 0.5	200 ± 10	2.0 ± 0.18	101 ± 11	25 ± 1.0	0.22 ± 0.01	111 ± 8
CsUDH158[d]	56.3 ± 0.3	−0.9 ± 0.5	219 ± 5	1.2 ± 0.01	186 ± 4	27 ± 1.5	0.14 ± 0.002	187 ± 11
A172 V (A)	60.9 ± 0.3	3.8 ± 0.4	225 ± 12	1.7 ± 0.16	136 ± 15	27 ± 1.7	0.18 ± 0.02	151 ± 23
M175 I (M)	58.6 ± 0.5	1.5 ± 0.6	153 ± 5	1.03 ± 0.02	149 ± 6	20 ± 0.4	0.18 ± 0.02	116 ± 12
D246 N (D)	63.8 ± 0.1	6.7 ± 0.4	192 ± 6	1.3 ± 0.05	146 ± 7	22 ± 1.1	0.18 ± 0.03	126 ± 19
CsUDH mutation combinations								
TAM	66.1 ± 0.1	9.0 ± 0.4	119 ± 5	1.1 ± 0.02	111 ± 5	19 ± 0.91	0.18 ± 0.03	104 ± 18
TMD	67.5 ± 0.2	10.4 ± 0.4	179 ± 3	1.1 ± 0.07	164 ± 11	29 ± 0.74	0.19 ± 0.01	155 ± 9
TAD	68.6 ± 0.1	11.4 ± 0.4	214 ± 6	1.5 ± 0.03	139 ± 5	30 ± 1.24	0.22 ± 0.01	138 ± 7
TAMD	71.4 ± 0.4	14.2 ± 0.5	130 ± 10	0.95 ± 0.05	138 ± 13	22 ± 0.84	0.18 ± 0.02	125 ± 17
CsUDH99.Y.TAMD	73.1 ± 0.03	16.0 ± 0.4	59 ± 1	0.43 ± 0.023	136 ± 8	20 ± 1.7	0.16 ± 0.01	126 ± 15
CsUDH-inc[e]	75.1 ± 0.3	17.9 ± 0.5	50 ± 2	0.65 ± 0.045	77 ± 6	17 ± 1.4	0.21 ± 0.01	78 ± 7

[a] $K_t^{0.5}$ = temperature at which ½ initial activity remains after 1 h incubation.
[b] CsUDHwt, Wild-type *Chromohalobacter salixigens* uronate dehydrogenase.
[c] Mutation CsUDH99 = N99 K, L100H, K102 V, P103 K, I105V.
[d] Mutation CsUDH158 = L158A, N159C, and I160 V.
[e] CsUDH-inc, *Chromohalobacter salixigens* uronate dehydrogenase containing all mutations in thermal stability screening hits (this study).

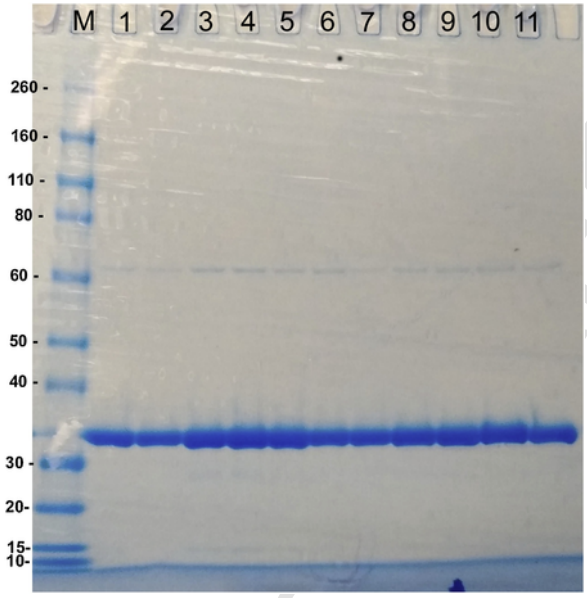

Fig. 2. SDS-PAGE analysis of CsUDH*wt* and mutant proteins.M, size markers (kD); 1, CsUDH*wt* (wild-type CsUDH); 2, T113 V (T); 3, A172 V (A); 4, M175 I (M); 5, D246 N (D); 6, TAM; 7, TMD; 8, TAD; 9, TAMD; 10, TAMD + N99K + L100H + K102V + P103K + I105V + Y116 F; 11, CsUDH-inc (contains all mutations this study Table 1).

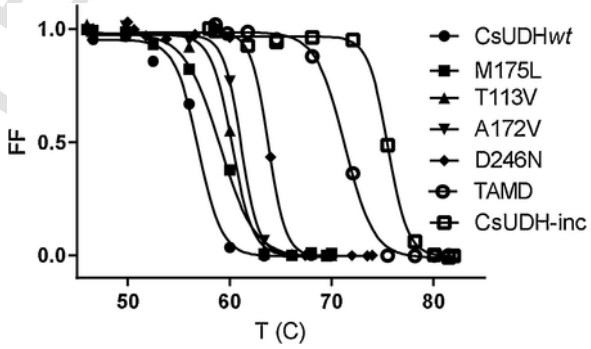

Fig. 3. Thermal denaturation profiles for CsUDHwt and selected mutants.CsUDHwt, wild-type *Chromohalobacter salixigens* uronate dehydrogenase; TAMD contains mutations T113 V, A172 V, M175 L, and D246 N; CsUDH-inc, *Chromohalobacter salixigens* uronate dehydrogenase containing all mutations in thermal stability screening hits (this study Table 1).

2.6. Protein crystallization and X-ray crystallography

Crystallization trials of CsUDH were initiated with a sample a concentration of 11 mg ml^{-1} in 40 mM Tris–HCl, pH 8.0, 50 mM NaCl, 1 mM DTT. The sample was screened with a Phoenix Robot (Art Robbins Instruments, Sunnyvale, CA) using the following crystallization screens: Natrix, Crystal Screen, PEG/Ion, Index, PEGRx (Hampton Research, Aliso Viejo, CA), and Berkeley Screen [32]. The CsUDH protein crystallized in several different crystal forms depending on crystallization conditions (Fig.4). The crystals from Berkeley Screen condition F9 were most suitable for structure determination and were analyzed further. The crystallization conditions for this trial were 0.1 M MES pH6.5 and 30 % 2-methyl-2-4-pentanediol (MPD). Crystals formed after 2 days by the sitting-drop vapor-diffusion method with the drops consisting of a mixture of 0.2 µl of protein solution and 0.2 µl of reservoir solution. The crystals were flash cooled in liquid nitrogen using cryoprotectant buffer matched to the crystallization reservoir solution. Single wavelength (1.0 Å) native X-ray diffraction data were collected at 100 K at Advanced Light Source at beamline 8.2.2, at Lawrence Berkeley National Laboratory. The mutant CsUDH-inc was solved from a single crystal that diffracted to 2.04 Å. The X-ray data were processed and indexed with xia2 [33]. Free-R flags were assigned to a random 5% of reflections and this test set was maintained throughout all subsequent stages of structure solution and refinement. The X-ray crystal structure of CsUDH was solved by molecular replacement using the program Phaser [34] using the PDBID:3AY3 as a starting model [35]. The real space refinement was carried out using PHENIX [36], and further refinement included translation/liberation/screw (TLS), and non-crystallographic symmetry constraints with several rounds of manual remodeling in COOT [37] between refinement cycles. B-value statistics for model comparison purposes

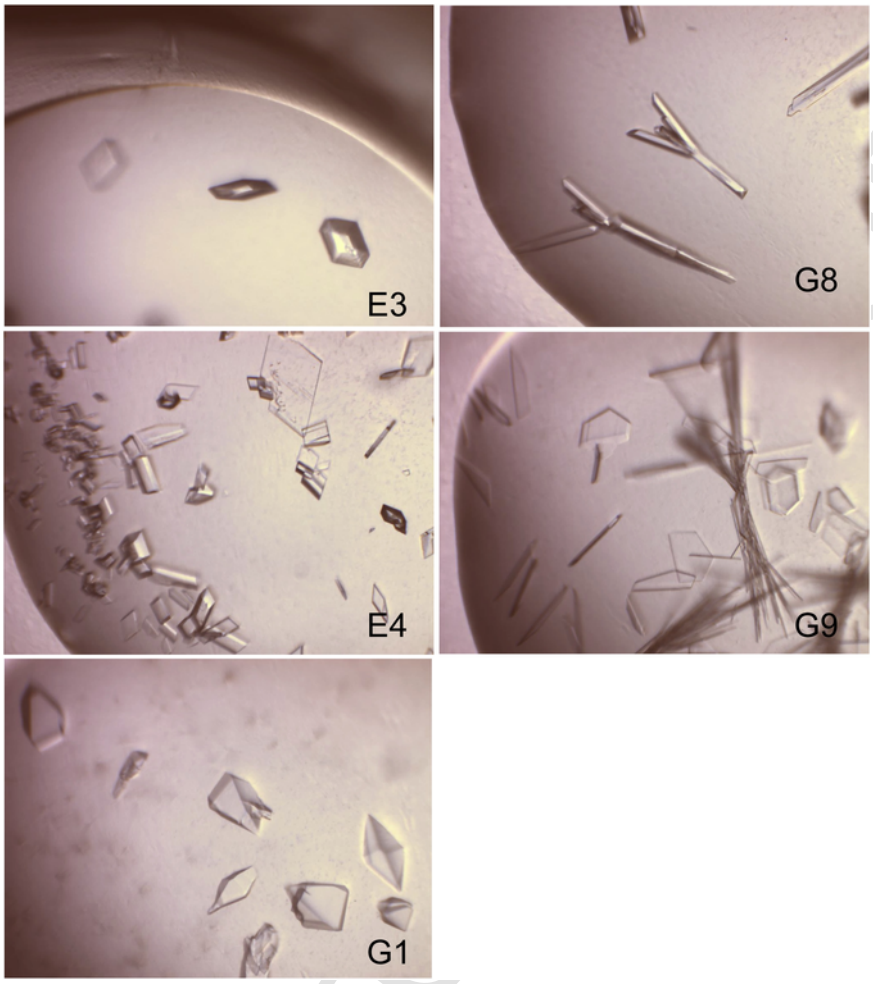

Fig. 4. CsUDH-inc crystals under various conditions.CsUDH-inc, *Chromohalobacter salixigens* uronate dehydrogenase containing all mutations in thermal stability screening hits (this study Table 1); E3, 0.1 M Sodium malonate pH 5.0 and 12 % polyethylene glycol (PEG) 3,350; E4, 0.2 M Sodium malonate pH 5.0 and 20 % PEG 3,350; G1, 0.1 M Sodium acetate pH 7.0 and 12 % PEG 3,350; G8, 2 % Tacsimate pH 5.0, 0.1 M Sodium citrate pH 5.6 and 16 % PEG 3,350; G9, 2 % Tacsimate pH 5.0, 0.1 M BIS-Tris pH 6.5 and 20 % PEG 3,350.

were computed using the CCP4 software suite [38]. The normalized B value is defined as B' = (B-<B>)/sig(B) where <B> is the mean B value in the structure and sig(B) the standard deviation (Fig. 5). The data collection and refinement statistics are summarized in Table 4. Model geometries were assessed with MolProbity as a part of the PHENIX validation tools [39]. Ramachandran statistics for the final refined structure are 98.17 % favored and 0 outliers. The fully refined structure has been deposited in the Protein Data Bank with the entry code 6MFH.

3. Results and discussion

Improved thermal stability of the enzyme components in an *in vitro* biosystem-based industrial process is important for increasing robustness, and moreover protein stability in general is important in allowing toleration of destabilizing mutations that can result as a protein structure is optimized for other properties or functions [40,41]. The amino acid sequence of the UDH from *Agrobacterium tumefaciens* (AtUDH) is 55 % identical and 67 % identical or similar to that of CsUDH (Fig. 1). AtUDH has been previously been engineered for improved thermal stability by a semi-rational approach designed to increase enzyme rigidity by focusing in part on mutagenesis of high B-factor amino acid residues [21]. We had previously characterized several UDH's and optimized the synthesized DNA sequences for homology for the DNA gene family shuffling efforts described here [30]. Thus, a gene family shuffled library was created from PsUDH, PnUDH, and CsUDH, with PsUDH having the lowest thermal stability and CsUDH the highest thermal stability, comprising a gene family with a large $\Delta K_t^{0.5}$ span of 23 °C with regards to intrinsic thermal stability [30]. Of 12,758 colonies in the initial 1° live/dead screen, 2969 23 %) were active. Retesting of hits from the 2° thermal screen for increased thermal stability resulted in five initial hits: 2F10, 16B3, 21F3, 2D11, and 33F2, with improved thermal stability $\Delta K_t^{0.5}$ values in the range 3.06 °C–8.00 °C (Table 1). Not surprisingly, the amino acid sequences of these hits are nearly identical (>98 %) with CsUDH, the parental enzyme with the greatest thermal stability. While DNA sequencing of randomly selected colonies from the shuffled library showed DNA mutations arising from recombination of all three gene parents, the initial hits selected by the thermal screening procedure contained a combined total of 27 DNA mutations arising from both CsUDH/PnUDH homologous recombination events and potentially PCR errors, with no codon mutations that could be uniquely ascribed to PsUDH recombination in any of the hits (data not shown). These 27 codon mutations resulted in 16 unique amino acid changes in total with respect to CsUDHwt, with the hits each containing from 2 to 9 amino acid substitutions (Table 1 and Fig.1). There were two areas of the protein where several mutations were clustered from homologous recombination with PnUDH that were treated as single mutation events in Table 2, these being denoted as CsUDH99, comprised by a loop between an α-helix and β-sheet containing 5 amino acid mutations, and CsUDH158, comprised of 3 amino acid mutations in a β-sheet (Table 1).

The effect of the mutation events both in isolation and in selected combinations on thermal stability $K_t^{0.5}$, and on kinetic parameters k_{cat} (25 °C) and K_m using both GluUA and GalUA as substrates was explored (Fig. 3, Tables 2 and 3). Of the ten mutation events examined in isolation, consisting of 8 single

Fig. 5. X-ray crystal structure of CsUDH-inc, Protein Data Bank accession 6MFH.CsUDH-inc, *Chromohalobacter salixigens* uronate dehydrogenase containing all mutations in thermal stability screening hits (this study Table 1).

Table 4
Csal-inc X-ray Crystal Structure Data collection and refinement statistics*.

Wavelength	1.0 Å	CC (work)	0.960 (0.758)
Resolution range	69.68 - 2.04 (2.113 - 2.04)	CC (free)	0.959 (0.791)
Space group	I 41 3 2	Number of non-hydrogen atoms	2440
Unit cell	197.098 197.098 197.098 90 90 90	Macromolecules	2161
Total reflections	1855367 (175836)	Ligands	34
Unique reflections	41593 (4107)	Solvent	245
Multiplicity	44.6 (42.8)	Protein residues	275
Completeness (%)	81.80 (81.74)	RMS (bonds)	0.005
Mean I/sigma(I)	15.36 (1.64)	RMS (angles)	1.03
Wilson B-factor	23.30	Ramachandran favored (%)	98.17
R-merge	0.4866 (3.457)	Ramachandran allowed (%)	1.83
R-meas	0.4921 (3.499)	Ramachandran outliers (%)	0.00
R-pim	0.0729 (0.5328)	Rotamer outliers (%)	0.88
CC1/2	0.997 (0.578)	Clash score	4.41
CC*	0.999 (0.856)	Average B-factor	33.69
Reflections used in refinement	34023 (3357)	Macromolecules	31.99
Reflections used for R-free	1635 (167)	Ligands	65.18
R-work	0.2060 (0.3285)	Solvent	44.35
R-free	0.2314 (0.3136)	Number of TLS groups	9

*Statistics for the highest-resolution shell are shown in parentheses.

amino acid mutations, the CsUDH99 loop mutation event (5 single amino acid mutations), and the CsUDH158 region mutation event (3 single amino acid mutations), only four mutations appreciably increased thermal stability with a $\Delta K_t^{0.5}$ range from +1.5 to +6.7 °C: T113 V, +3.1 °C (T), A172 V, +3.8 °C (A), M175 L, +1.5 °C (M), and D246 N, +6.7 °C (D), (Table 3, Fig.3). Interestingly, while mutations T, M, and D were from homologous recombination, mutation A appears to have arisen from a PCR or recombination error during either bulk DNA preparation or gene shuffling. For these mutated residues resulting in the most impact on thermal stability, mutations T, A, and M are all in the interior of the protein and well packed in the wild-type and mutant structures, and in fact are immediately adjacent to residues shown previously to be involved in substrate binding [35](Fig.1), while mutation D is on the surface near the peptide C-terminal and had the largest individual effect on thermal stability. The effect of substrate binding site on thermal stability has previously been observed where NAD^+, GluUA and GalUA all protected CsUDH from thermal denaturation [30]. For these four mutants (T, A, M, and D), k_{cat}(GluUA) was found to decrease by 17–42 % and k_{cat}(GluUA) by 12–35 %, while K_m values were not significantly affected for either substrate, except K_m (GluUA) for the M175 l mutant was lower, though the large uncertainty in K_m for CsUDHwt renders this latter observation tentative. Mutations CsUDH99 and I114 T also showed large decreases in k_{cat} for both GluUA and GalUA, and I114 T was interesting in also doubling K_m for either substrate. It should be noted here that substrate concentrations could be expected to be high for industrial *in vitro* application of the enzyme, with reaction velocity being dependent on k_{cat} and thus not affected by an increase in K_m since the enzyme would be operating under saturating substrate concentrations. Moreover, an increase in K_m as seen for the I114 T mutant may be beneficial since CsUDH was shown to exhibit substrate inhibition, and an increase in K_m has been shown to lessen substrate inhibition by simultaneously increasing K_{si}, the dissociation constant for substrate and enzyme, in previous directed evolution studies of a xylosidase enzyme [30,42].

Saturation mutagenesis was performed for sites M175 and D246 (Table 2), where for site M175 only 11 of 19 alternative peptides resulted in detectable activity, while for position D246 only mutation to Pro resulted in no activity being detected. The observed inactivity of some mutations at these positions is likely due to either absent or prohibitively low catalytic turnover alone, or in combination with reduced or absent protein expression. Position M175 being in the interior of the protein adjacent to substrate binding residues thus appears to be more sensitive to amino acid mutation than position D246 located on the surface near the C-terminus. Also, at position M175 the 11 apparently allowable mutations such that activity could be determined all decreased $\Delta K_t^{0.5}$ by at least 9 °C and by as much as 20 °C, with the sole exception of the thermally stabilizing mutation M175 l that was selected, which arose from CsUDH/PnUDH recombination. For position D246, all mutations except Pro were apparently allowed, with the native Asp residue being among the three most thermally unstable residues at this position. Thus, nearly all mutations of D246 increased thermal stability, though by a smaller ~ 8 °C range than seen for position M175 saturation mutagenesis, with the selected mutation D246 N being one of the most thermally stabilizing residues at this position.

Combining the 4 mutations in enzyme TAMD (Table 3, Fig.3) showed that the mutations were additive within experimental error [43,44], resulting in $\Delta K_t^{0.5}$ = +14.2 °C. Mutant TAMD compared to CsUDHwt showed k_{cat}(GluUA) halved and that for GalUA decreased by ~1/3, with K_m(GalUA) unchanged and K_m(GluUA) decreased. Adding mutations CsUDH99 and Y116 F to TAMD (Table 3) further increased thermal stability by 1.8 °C, with a 35 % k_{cat}(GalUA) and 78 % k_{cat} (GluUA) reduction, while a ~4-fold reduction in K_m (GluUA) was observed and K_m (GalUA) was unchanged. Finally, the thermal stability of enzyme CsUDH-inc, containing all mutations, the majority of which in isolation are neutral with respect to thermal stability, when combined increase the thermal stability of TAMD an additional 3.7 °C ($\Delta K_t^{0.5}$ = ~ +18 °C); such an increase in thermal stability with singularly neutral mutation addition has previously been noted for AtUDH [21]. Thus, for CsUDH-inc the temperature at which the enzyme begins to denature after 1 h was improved by ~15 °C from ~50–55 °C to ~ 75 °C (Fig. 2), k_{cat} (GluUA) was decreased ~five-fold, and k_{cat} (GalUA) was less affected, being ~ ½ that of CsUDHwt.

For application in an industrial process, increasing or maintaining k_{cat} while improving thermal stability is desirable, and to address the observed k_{cat} reduction with increasing mutation without also selecting for activity, as noted previously for enzyme stability engineering campaigns [29,45], a series of less-mutated enzymes TMD, TAD, TAM were constructed containing 3 of the 4 most influential single mutations for thermal stability. Mutant TAD was appreciably more thermal stable with $\Delta K_t^{0.5}$ = +11.4 °C (~69 °C), with k_{cat} (GluUA) de-

Thus, for oxidation of GalUA, mutant TAD significantly improves upon the thermal stability of CsUDHwt with good activity using GluUA, and k_{cat}(GalUA) was comparable to CsUDHwt. TAD thermostability is comparable to that recently described for the UDH enzyme from the thermophilic organism *Thermobispora bispora* (amino acid sequence 42 % identical and 59 % identical or similar to CsUDH), which retains 58 % of initial activity after 1 h at 60 °C [46].

The most thermally stabilized enzyme CsUDH-inc was crystallized (Fig. 4), and the x-ray crystal structure was determined to 1.9 Å resolution (PDB = 6MFH; Table 4). Analysis of the crystal structure (Fig. 5) revealed the molecule crystallized as a hexamer, comprised of a trimer of dimers, consistent with the quaternary structure observed previously in solution using size-exclusion chromatography (SEC) based on hydrodynamic radius, where a nearly heptameric (6.6) quaternary structure was observed [30]. The closely related enzyme AtUDH also crystalized as a trimer of dimers and also existed in solution as a hexamer [47].

In previous gene family shuffling DE studies of xylosidase enzymes SXA and XylBH43, a L186Ymutation in XylBH43 shown to improve $K_t^{0.5}$ derived from homologous recombination with SXA (52 % identical, 62 % identical or homologous) was further interrogated by saturation mutagenesis, with Lys being optimal at that position for increasing thermal stability. However, when the native Tyr residue at that position in SXA was mutagenized to Lys to test the transferability of the effect, Lys instead diminished $K_t^{0.5}$ by 2.4 °C [31]. On the other hand, mutation W145 G in SXA found to diminish substrate and product inhibition when tested in XylBH43 [48], had a similar effect in that enzyme [49]. Thus mutational effects appear to be context dependent, and in the present study it is not clear that the identification of thermal stability enhancing mutations in CsUDH necessarily pertains to analogous positions in homologous UDH enzymes such as AtUDH.

The B-factors derived from the X-ray crystal structure are considered temperature factors that correlate with crystalline state electron density fluctuation due to thermal motion [50]. In ordering amino acid residue B-factor values previously determined for the crystal structure of CsUDHwt [35], from highest B-factor and greatest thermal motion in the crystal structure = #1 to lowest B-factor = #267, residues TAMD were ranked 265/267, 130/267, 175/267, and 59/267, respectively. Thus, indeed residue D246 had a highly ranked B-factor, and moreover its mutation clearly imparted the greatest individual contribution to thermal stabilization among selected mutations, lending credence to increased scrutiny of such residues in an enzyme thermal engineering strategy. However, it should also be noted that here in most cases the B-factor of the residue appeared to not be of primary importance for thermal stability selection; T113 has nearly the smallest B-factor in the entire peptide chain, yet when mutated had an appreciable effect on thermal stability. An analyses of the thermal displacement parameters of the wild type and the mutant structure do not indicate significant changes in the stability in cryogenic structure apart from an overall increase in B value for the wild type which can be ascribed to less optimal crystallization conditions or cryogenic freezing of the samples (Fig. 6). Future high-resolution room temperature studies could provide additional structural insights into the observed stability increase.

4. Conclusion

CsUDH-inc was found have $\Delta K_t^{0.5}$ significantly improved by ~18 °C after just one round of gene family shuffling and combination of mutations, with activity being unaffected by incubation for 1 h at ~70 °C. While activity of CsUDH-inc was severely reduced, constructs containing 3 mutations were identified that retained good activity with $\Delta K_t^{0.5}$ = +10°. Residues most affecting thermal stability were clustered immediately adjacent to residues thought to be involved in substrate binding. Interestingly, comparison of rescaled B-factors obtained for the protein containing all mutations with the values obtained for the wild type enzyme showed no obvious differences.

CRediT authorship contribution statement

Kurt Wagschal: Conceptualization, Formal Analysis, Data Curation, Visualization, Writing-original draft, Writing - review & editing. **Victor J. Chan:** Methodology, Investigation, Resources, Formal Analysis, Visualization, Writing - original draft. **Jose H. Pereira:** Methodology, Investigation, Resources, Visualization, Writing-original draft. **Peter H. Zwart:** Conceptualization, Methodology, Formal Analysis, Visualization, Writing-original draft, Writing-review & editing. **Banumathi Sankaran:** Conceptualization, Methodology, Investigation, Formal Analysis, Visualization, Writing-original draft, Writing-review & editing.

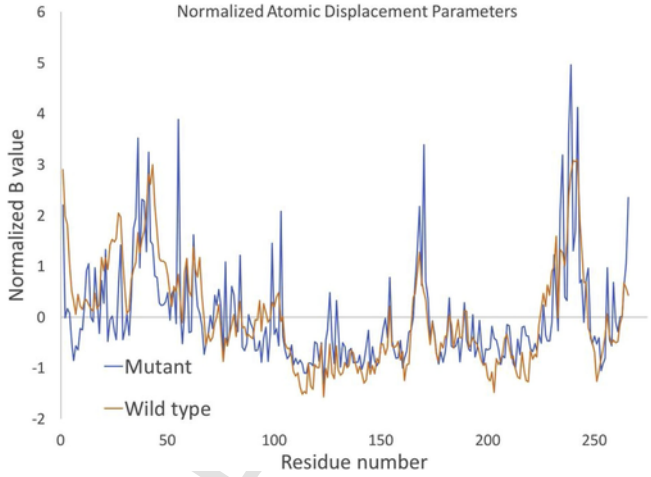

Fig. 6. Comparison of rescaled B-values for Mutant (CsUDH-inc) and Wild type (CsUDHwt).CsUDH-inc, *Chromohalobacter salixigens* uronate dehydrogenase containing all mutations in thermal stability screening hits (this study Table 1), Protein Data Bank accession 6MFH; CsUDHwt, wild-type *Chromohalobacter salixigens* uronate dehydrogenase, Protein Data Bank accession 3AY3.

Declaration of Competing Interest

None.

Acknowledgments

This work was supported by the United States Department of Agriculture CRIS 5325-41000-054-00D (V.J.C. and K.W.). The ALS-ENABLE beamlines are supported in part by the National Institutes of Health, National Institute of General Medical Sciences, grant P30 GM124169-01 and the Howard Hughes Medical Institute (B.S.). The Advanced Light Source is a Department of Energy Office of Science User Facility under Contract No. DE-AC02-05CH11231. The mention of firm names or trade products does not imply that they are endorsed or recommended by the US Department of Agriculture over other firms or similar products not mentioned. USDA is an equal opportunity provider and employer.

References

[1] C.S.K. Lin, L.A. Pfaltzgraff, L. Herrero-Davila, E.B. Mubofu, S. Abderrahim, J.H. Clark, et al., Food waste as a valuable resource for the production of chemicals, materials and fuels. Current situation and global perspective, Energy and Environ. Sci. 6 (2) (2013) 426–464.
[2] E.S. Bernhardt, E.J. Rosi, M.O. Gessner, Synthetic chemicals as agents of global change, Front. Ecol. Environ. 15 (2) (2017) 84–90.
[3] F. Creutzig, Govern land as a global commons, Nature 546 (7656) (2017) 28–29.
[4] K. Rezzadori, S. Benedetti, E.R. Amante, Proposals for the residues recovery: orange waste as raw material for new products, Food Bioprod Process 90 (4) (2012) 606–614.
[5] T.L.H. Treuer, J.J. Choi, D.H. Janzen, W. Hallwachs, D. Peréz-Aviles, A.P. Dobson, et al., Low-cost agricultural waste accelerates tropical forest regeneration, Restor Ecol 26 (2) (2018) 275–283.
[6] B.M. Yapo, P. Lerouge, J.-F. Thibault, M.-C. Ralet, Pectins from citrus peel cell walls contain homogalacturonans homogenous with respect to molar mass, rhamnogalacturonan I and rhamnogalacturonan II, Carbohydr. Polym. 69 (3) (2007) 426–435.
[7] J. Doran-Peterson, D.M. Cook, S.K. Brandon, Microbial conversion of sugars from plant biomass to lactic acid or ethanol, Plant J. 54 (4) (2008) 582–592.
[8] A. Inoue, T. Ojima, Functional identification of alginate lyase from the brown alga Saccharina japonica, Sci. Rep. 9 (1) (2019) 4937.

[9] H. Boer, H. Maaheimo, A. Koivula, M. Penttilä, P. Richard, Identification in Agrobacterium tumefaciens of the D-galacturonic acid dehydrogenase gene, Appl. Microbiol. Biotechnol. 86 (2010) 901–909.
[10] T. Werpy, G. Petersen, Top Value Added Chemicals From Biomass, Volume 1-results of Screening for Potential Candidates From Sugars and Synthesis Gas, US dept of energy, Washington DCin: http://www1.eere.energy.gov/bioenergy/pdfs/35523.pdf, 2004, 1.
[11] A. Abbadi, K.F. Gotlieb, J.B.M. Meiberg, J.A. Peters, H. Van Bekkum, New Ca-sequestering materials: based on the oxidation of the hydrolysis products of lactose, Green Chem. 1 (5) (1999) 231–235.
[12] T. Mehtiö, M. Toivari, M.G. Wiebe, A. Harlin, M. Penttilä, A. Koivula, Production and applications of carbohydrate-derived sugar acids as generic biobased chemicals, Crit. Rev. Biotechnol. 36 (5) (2016) 904–916.
[13] H. Zhang, X. Li, X. Su, E.L. Ang, Y. Zhang, H. Zhao, Production of adipic acid from sugar beet residue by combined biological and chemical catalysis, Chem. Cat. Chem 8 (8) (2016) 1500–1506.
[14] E. Shiue, K.L.J. Prather, Improving d-glucaric acid production from myo-inositol in E. Coli by increasing MIOX stability and myo-inositol transport, Metab. Eng. 22 (2014) 22–31.
[15] J. Kuivanen, Y.M.J. Wang, P. Richard, Engineering Aspergillus niger for galactaric acid production: elimination of galactaric acid catabolism by using RNA sequencing and CRISPR/Cas9, Microb. Cell Fact. 15 (2016) 210.
[16] R.J. Protzko, L.N. Latimer, Z. Martinho, E. de Reus, T. Seibert, J.P. Benz, et al., Engineering Saccharomyces cerevisiae for co-utilization of d-galacturonic acid and d-glucose from citrus peel waste, Nat. Commun. 9 (1) (2018) 5059.
[17] Y. Lu, Cell-free synthetic biology: engineering in an open world, Synth. Syst. Biotechnol. 2 (1) (2017) 23–27.
[18] Y.H.P. Zhang, Production of biofuels and biochemicals by in vitro synthetic biosystems: opportunities and challenges, Biotechnol. Adv. 33 (7) (2015) 1467–1483.
[19] A. Pick, J. Schmid, V. Sieber, Characterization of uronate dehydrogenases catalysing the initial step in an oxidative pathway, Microbial Biotechnol 8 (2015) 633–643.
[20] D. Mojzita, M. Wiebe, S. Hilditch, H. Boer, M. Penttilä, P. Richard, Metabolic engineering of fungal strains for conversion of D-galacturonate to meso-Galactarate, Appl. Environ. Microbiol. 76 (1) (2010) 169–175.
[21] T. Roth, B. Beer, A. Pick, V. Sieber, Thermostabilization of the uronate dehydrogenase from Agrobacterium tumefaciens by semi-rational design, AMB Express 7 (1) (2017) 103.
[22] C.R. Darwin, A.R. Wallace, On the tendency of species to form varieties: and on the perpetuation of varieties and species by means of selection, J. Proc. Linnean Soc. London, Zoology 3 (1858) 45–62.
[23] K. Chen, F.H. Arnold, Enzyme engineering for nonaqueous solvents: random mutagenesis to enhance activity of subtilisin e in polar organic media, BioTechnology 9 (1991) 1073–1077.
[24] F.H. Arnold, Directed evolution: bringing new chemistry to life, Angewandte Chemie - International Edition 57 (16) (2018) 4143–4148.
[25] J.-H. Zhang, G. Dawes, W.P.C. Stemmer, Directed evolution of a fucosidase from a galactosidase by DNA shuffling and screening, Proc Natl Acad Sci 94 (1997) 4504–4509.
[26] R.J. Fox, G.W. Huisman, Enzyme optimization: moving from blind evolution to statistical exploration of sequence-function space, Trends Biotechnol. 26 (3) (2008) 132–138.
[27] W.P.C. Stemmer, DNA shuffling by random fragmentation and reassembly: in vitro recombination for molecular evolution, Proc. Natl. Acad. Sci. 91 (1994) 10747–10751.
[28] A. Crameri, S.-A. Raillard, E. Bermudez, W.P.C. Stemmer, DNAshuffling of a family of genes from diverse species accelerates directed evolution, Nature 391 (1998) 288–291.
[29] L. Giver, A. Gershenson, P.-O. Freskgard, F.H. Arnold, Directed evolution of a thermostable esterase, Proc. Natl. Acad. Sci. 95 (1998) 12809–12813.
[30] K. Wagschal, D.B. Jordan, C.C. Lee, A. Younger, J.D. Braker, V.J. Chan, Biochemical characterization of uronate dehydrogenases from three Pseudomonads, Chromohalobacter salixigens, and Polaromonas naphthalenivorans, Enzyme Microb. Technol. 69 (2015) 62–68.
[31] S.K. Singh, C. Heng, J.D. Braker, V.J. Chan, C.C. Lee, D.B. Jordan, et al., Directed evolution of GH43 β-xylosidase XylBH43 thermal stability and L186 saturation mutagenesis, J. Ind. Microbiol. Biotechnol. 41 (3) (2014) 489–498.
[32] J.H. Pereira, R.P. McAndrew, G.P. Tomaleri, Adams PD. Berkeley Screen: a set of 96 solutions for general macromolecular crystallization, J. Appl. Crystallogr. 50 (5) (2017) 1352–1358.
[33] G. Winter, Xia2: An expert system for macromolecular crystallography data reduction, J. Appl. Crystallogr. 43 (1) (2010) 186–190.
[34] A.J. McCoy, R.W. Grosse-Kunstleve, P.D. Adams, M.D. Winn, L.C. Storoni, R.J. Read, Phaser crystallographic software, J. Appl. Crystallogr. 40 (4) (2007) 658–674.
[35] J.W. Ahn, S.Y. Lee, S. Kim, S.M. Kim, S.B. Lee, K.J. Kim, Crystal structure of glucuronic acid dehydrogeanse from Chromohalobacter salexigens, Proteins Struct. Funct. Bioinform. 80 (1) (2012) 314–318.
[36] P.D. Adams, P.V. Afonine, G. Bunkóczi, V.B. Chen, I.W. Davis, N. Echols, et al., PHENIX: a comprehensive Python-based system for macromolecular structure solution, Acta Crystallogr Sect D Biol Crystallogr 66 (2) (2010) 213–221.
[37] P. Emsley, B. Lohkamp, W.G. Scott, K. Cowtan, Features and development of coot, Acta Crystallogr Sect D Biol Crystallogr 66 (4) (2010) 486–501.
[38] M.D. Winn, C.C. Ballard, K.D. Cowtan, E.J. Dodson, P. Emsley, P.R. Evans, et al., Overview of the CCP4 suite and current developments, Acta Crystallographica Section D 67 (4) (2011) 235–242.
[39] V.B. Chen, W.B. Arendall Iii, J.J. Headd, D.A. Keedy, R.M. Immormino, G.J. Kapral, et al., MolProbity: all-atom structure validation for macromolecular crystallography, Acta Crystallogr Sect D Biol Crystallogr 66 (1) (2010) 12–21.
[40] J.D. Bloom, S.T. Labthavikul, C.R. Otey, F.H. Arnold, Protein stability promotes evolvability, Proc Natl Acad Sci 103 (2006) 5869–5874.
[41] N. Ota, R. Kurahashi, S. Sano, K. Takano, The direction of protein evolution is destined by the stability, Biochimie 150 (2018) 100–109.
[42] D.B. Jordan, K. Wagschal, Z. Fan, L. Yuan, J.D. Braker, C. Heng, Engineering lower inhibitor affinities in β-D-xylosidase of Selenomonas ruminantium by site-directed mutagenesis of Trp145, J. Ind. Microbiol. Biotechnol. 38 (2011) 1821–1835.
[43] M. Matsumura, S. Yasumura, S. Aiba, Cumulative effect of intragenic amino-acid replacements on the thermostability of a protein, Nature 323 (1986) 356–358.
[44] J.A. Wells, Additivity of mutational effects in proteins, Biochemistry 29 (37) (1990) 8509–8517.
[45] S.R. Miller, An appraisal of the enzyme stability-activity trade-off, Evolution 71 (7) (2017) 1876–1887.
[46] Y. Li, Y. Xue, Z. Cao, T. Zhou, F. Alnadari, Characterization of a uronate dehydrogenase from Thermobispora bispora for production of glucaric acid from hemicellulose substrate., World J. Microbiol. Biotechnol. 34 (7) (2018) 102.
[47] T. Parkkinen, H. Boer, J. Janis, M. Andberg, M. Penttila, A. Koivula, et al., Crystal structure of uronate dehydrogenase from Agrobacterium tumefaciens, J. Biol. Chem. 286 (31) (2011) 27294–27300.
[48] Z. Fan, L. Yuan, D.B. Jordan, K. Wagschal, C. Heng, J.D. Braker, Engineering lower inhibitor affinities in β-xylosidase, Appl. Microbiol. Biotechnol. 86 (2010) 1099–1113.
[49] K. Wagschal, D.B. Jordan, J.D. Braker, Catalytic properties of β-D-xylosidase XylBH43 from Bacillus halodurans C-125 and mutant XylBH43-W147G, Process Biochem. 47 (2012) 366–372.
[50] Z. Yuan, J. Zhao, Z.-X. Wang, Flexibility analysis of enzyme active sites by crystallographic temperature factors, Protein Eng. Des. Sel. 16 (2) (2003) 109–114.